

Assessing and mitigating systematic errors in forest attribute maps utilizing harvester and airborne laser scanning data

Janne Rätty*, Marius Hauglin, Rasmus Astrup, Johannes Breidenbach*

Norwegian Institute of Bioeconomy Research (NIBIO), National Forest Inventory, Høgskoleveien 8, 1433 Ås, Norway

*Corresponding authors:

[firstname].[lastname]@nibio.no

Abstract

Cut-to-length harvesters collect useful information for modeling relationships between forest attributes and airborne laser scanning (ALS) data. However, harvesters operate in mature forests, which may introduce selection biases and systematic errors in harvester data-based forest attribute maps. We fitted regression models (harvester models) for volume (V), height (HL), stem frequency (N), above-ground biomass, basal area, and quadratic mean diameter (QMD) using harvester and ALS data. The performances of the harvester models were evaluated using Norwegian national forest inventory plots in an 8.7Mha study area. We estimated the bias of large-area synthetic estimators and compared efficiencies of model-assisted (MA) estimators with field data-based estimators. The harvester models performed better in productive than unproductive forests, but systematic errors occurred in both. The use of the MA estimators resulted in efficiency gains that were the largest for HL (relative efficiency, RE=6.0) and the smallest for QMD (RE=1.5). The bias of the synthetic estimator was largest for N (39%) and smallest for V (1%). The latter was due to an overestimation of deciduous and an underestimation of spruce forest that by chance balanced. We conclude that a probability sample of reference observations may be required to ensure the unbiasedness of estimators utilizing harvester data.

Key words: Cut-to-length harvester data, model-assisted estimation, national forest inventory, airborne lidar, large-area estimation

1 Introduction

The increased availability of wall-to-wall ALS data during the past 20 years has revolutionized the mapping of forest resources (Maltamo et al., 2021). Several countries all over the world have thus established ALS-based approaches for the wall-to-wall mapping of forest resources (Asner et al., 2012; Hauglin et al., 2021; Maltamo and Packalen, 2014; Nilsson et al., 2017; Nord-Larsen et al., 2017; White et al., 2013). Operationally utilized forest attribute maps are primarily constructed using the area-based approach (ABA), which relies on a statistical modeling using a sample of field plots and ALS data collected from an area of interest (Næsset, 2014, 1997). Field data collection account for a considerable proportion of forest inventory costs, and several alternatives to reduce the inventory costs have been investigated (Noordermeer et al., 2019; Rahlf et al., 2021; Tompalski et al., 2019).

Due to high efficiency and safety for forest workers, close to 100 % of all commercial forest harvests are today conducted using cut-to-length harvesters in the Nordic countries. Harvesters collect huge amounts of data about the harvested trees which, so far, are under-utilized in forest inventories and the forest value chain (Kemmerer and Labelle, 2020). Harvester data are a potential alternative to traditional field data in forest inventories relying on airborne laser scanning (ALS). In addition to the economic efficiency of data collection, harvester data are also attractive since these data include bucking information (Bollandsås et al., 2013; Karjalainen et al., 2019; Rätty et al., 2021b). Harvesters also enable the collection of data from large area units that are too expensive to measure using traditional field measurements. For example, complete descriptions of forest stands are valuable for the validation of remote sensing-based forest attribute maps (Vähä-Konka et al., 2020).

Several studies have suggested that harvester data are useful in ALS-based forest inventories. Hauglin et al. (2018) predicted timber volume using different regression techniques using harvester and ALS data in Norway. They compared the harvester data-based models with models based on traditional field measurements. They reported that root-mean-square errors (RMSEs) associated with timber volume predictions were similar regardless of training data. They, however, only evaluated their models using cross-validation. Söderberg et al. (2021) studied the operational applicability of harvester data in the ALS-based forest inventories in Sweden. They predicted several stand-level forest attributes such as merchantable volume, basal area and tree size distributions using the k nearest neighbor approach. Maltamo et al. (2019) also used harvester data and ALS data to predict stand-level diameter distributions and several forest attributes, such as merchantable volume and basal area, using the k nearest neighbor approach. Noordermeer et al. (2022) mapped and estimated merchantable timber volume at the level of grid cells and harvested sites (i.e., a cluster of adjacent stands) using harvester and ALS data. They studied the effect of tree positioning errors and the size of modeling units on the predictive performance of the models. Saukkola et al. (2019) also studied the effect of tree positioning errors on the predictive performances of the models and found that the negative effects of inaccurate tree positioning on predictive performance can be mitigated by increasing the size of modeling unit. This conclusion is in line with the findings by Noordermeer et al. (2022).

There are also a few limitations associated with the use of harvester data in forest inventories. In Norway, harvesters are most often used to carry out final harvests (i.e. clear-cuts) in commercially mature forests. This means that the forest data collected by harvesters are typically biased towards mature forests. Commercial maturity implies that harvested forests are actively managed according to current silvicultural recommendations. The silvicultural operations used to

optimize timber production during a rotation period may reflect the size distribution of trees and composition of tree species in forest stands. Another limitation of harvester data is that even final harvests do not always mean that trees are completely removed from the forest stands. For example, retention trees or retention tree groups are usually left out of the final harvests, because they can mitigate negative effects of final harvests on biodiversity (Fedrowitz et al., 2014). Retention trees and selective harvests cause incompatibilities between harvester and ALS data. Currently, harvesters do not routinely record trees left out of harvest operations.

Wall-to-wall forest attribute maps are typically utilized for the purposes of stand-level forest management, whereas large-area estimations relying on national forest inventories (NFIs) are based on a probability sample ensuring unbiased forest attribute estimates (Kangas and Maltamo, 2006). Model-assisted (MA) estimation combines forest attribute maps and a probability sample in order to yield unbiased estimates with improved precision compared with direct estimation (Breidenbach et al., 2020b; McRoberts et al., 2017; Saarela et al., 2015). If a sufficient probability sample is not available, it is also possible to rely solely on the underlying model and summarize the pixels of a wall-to-wall forest attribute map to obtain large-area estimates (Ceccherini et al., 2020). These so-called synthetic estimates which are also known as “pixel-counting” estimates (Waldner and Defourny, 2017), may however hold systematic errors, if the model underlying the map is insufficient (Breidenbach et al., 2021a; Palahí et al., 2021). Systematic errors in estimates hamper decision making aiming at the optimal planning and management of forest resources (Ruotsalainen et al., 2021).

Harvester data can be a cost-efficient data source for the mapping and estimation of forest attributes in the ABA forest inventories relying on ALS data. However, it is not well understood

how large systematic errors are when such forest attribute maps are used for large-area mapping and estimation. Therefore, our objectives were

- (1) to study the predictive performance of models fit using harvester and ALS data (harvester models) using independent test data (NFI field plots),
- (2) to study the magnitude of systematic errors in synthetic estimates derived from forest attribute maps that result from harvester models,
- (3) to compare the precisions of the MA estimates (combination of synthetic estimates and NFI data) to direct estimates (only NFI data) in an 8.7 Mha study area in Norway.

The forest attributes of interest in this study were timber volume (V), Lorey's height (HL), stem frequency (N), above-ground biomass (AGB), basal area (G), and quadratic mean diameter (QMD).

2 Material and Methods

2.1 Study area

The 8.7 Mha study area is located between the latitudes of 58.0°N and 66.1°N in Norway (Figure 1) and comprises forests below the coniferous limit defined as the lowland stratum in the Norwegian NFI (Breidenbach et al., 2020a). Forests cover 84 % of the study area according to the NFI definition of the ability to reach 10 % crown cover and 5 m height. Norway spruce (*Picea abies* [L.] Karst.) is the dominating tree species and comprise 48 % of total volume in the study area. Scots pine (*Pinus sylvestris* [L.]) is especially common on sites that are not fertile enough for Norway spruce. Deciduous trees, mostly birch (*Betula spp.*) typically grow as

mixtures among coniferous species. Scots pine and deciduous species comprise 33 % and 19 % of total volume, respectively.

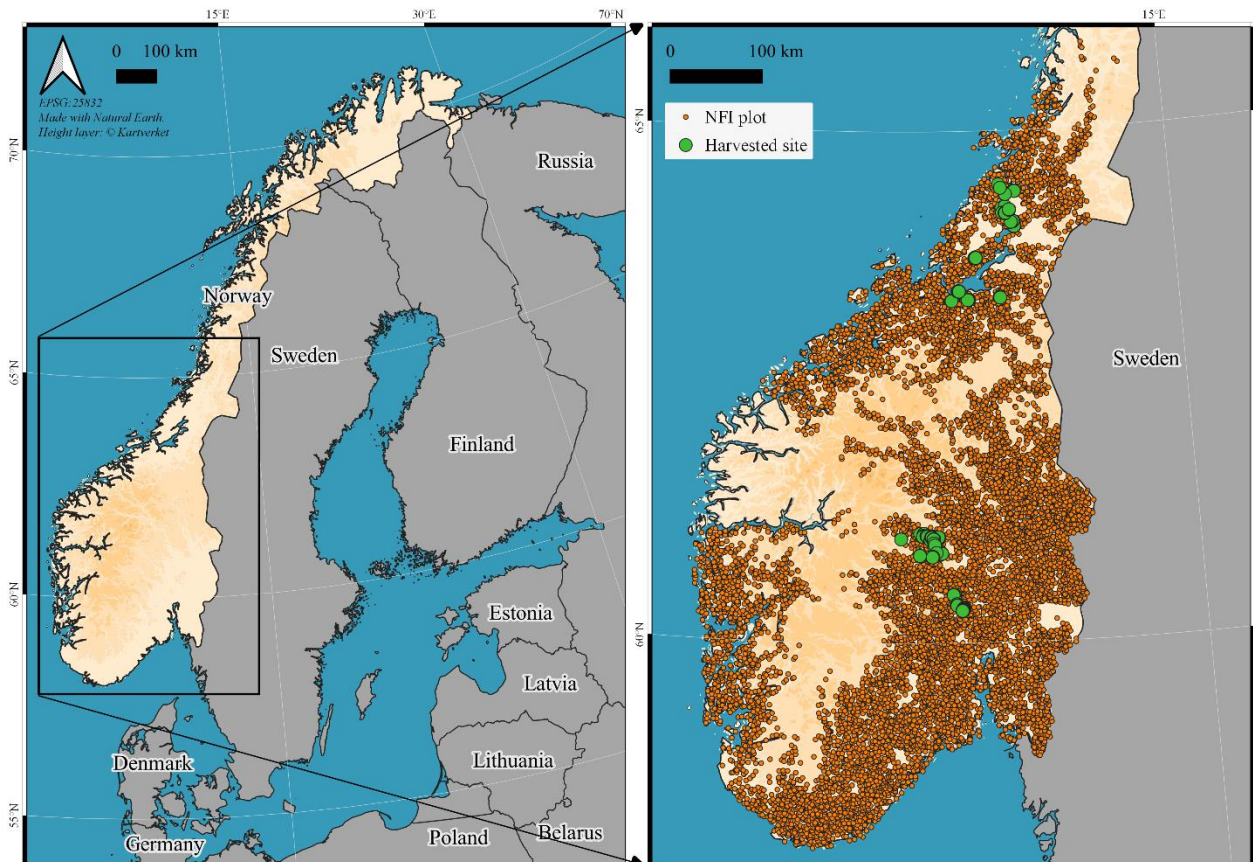


Figure 1. Approximate location of national forest inventory (NFI) plots and harvested sites in the study area.

2.2 National forest inventory data

The Norwegian NFI follows a systematic grid of 3 km × 3 km in the lowland stratum and the plots are located at the grid knots. The NFI plots are circular with a fixed area of 250 m², where all trees with diameter at breast height (DBH) ≥ 5 cm are recorded. Tree heights are recorded for a subset of approximately 10 trees per plot. The heights of remaining trees, as well as volume and biomass for each tree, are predicted using tree-level height-diameter, V, and AGB models. A

detailed description of the sampling design and measurement protocol of the Norwegian NFI is given by (Breidenbach et al., 2020a).

In this study, the plot-level forest attributes HL, V, N, AGB, G, and QMD were variables of interest. The stand-level attributes site index, i.e. height in the age of 40 (Tveite, 1977; Tveite and Braastad, 1981) and maturity class (M1, ..., M5) (Breidenbach et al., 2020a) were used to specify data domains in which model performances were evaluated. The maturity classification indicates the development stage of forest which depends on age, site index and tree species. The maturity classes are determined in terms of forest age as follows:

- M1: Forest under regeneration (age 0 yrs.)
- M2: Young forest (age 1–54 yrs.)
- M3: Young production forest (age 15–84 yrs.)
- M4: Older production forest (age 25–119 yrs.)
- M5: Mature forest (minimum age 40–120 yrs.)

Typically, most of the commercial harvests in Norway are expected to occur in maturity classes M4 and M5.

The NFI data within the study area comprise of 9,615 plots that were measured between 2016 and 2020. We excluded 305 plots where harvests occurred between field measurements and ALS data acquisition. All 9,310 plots covering all land uses constitute estimation data that were used in large-area estimation (Section 2.7). A total of 7,841 plots were located in forest.

Furthermore, the NFI data were used to establish two test data to evaluate the predictive performances of the harvester models: (1) test data that included all forest plots (ALL), and (2)

test data that included productive forests (PROD). Forests under regeneration (M1) were not included in the test data because they are typically covered trees below the caliper threshold. We utilized attributes of the NFI data to select NFI plots that are presumably in productive managed forests which are likely to be clear felled by harvesters in the future. Site index (> 11), coniferous volume proportion ($> 80\%$) and forwarding distance to the closest road (< 500 m) were used as criteria to determine plots that are in productive forests. Both test data only included plots that were completely on forest land. The ALL and PROD data comprise 5,858 and 614 NFI plots, respectively. Statistics associated with the ALL and PROD data are shown in Table 1. We present the statistics by maturity classes since the maturity classification was utilized in the performance evaluation of the models.

Table 1. Means and standard deviations (SDs) of forest attributes in the test data (ALL and PROD) that consist of national forest inventory (NFI) data. The ALL and PROD data comprise all forest and productive forest plots, respectively. V – volume, HL – Lorey’s height, N – stem frequency, AGB – above-ground biomass, G – basal area, QMD – quadratic mean diameter, M2, ..., M5 – NFI maturity classification (see section 2.2).

Data		ALL	PROD	ALL	PROD	ALL	PROD	ALL	PROD	ALL	PROD
Maturity class		M2– M5		M2		M3		M4		M5	
HL (m)	Mean	13.4	15.8	9.6	9.2	12.3	13.9	14.9	18.8	14.8	22.1
	SD	4.4	4.8	3.7	3.6	3.2	3.0	4.3	3.0	4.2	4.0
V (m ³ · ha ⁻¹)	Mean	149.4	226.2	41.7	49.1	134.6	175.6	199.9	309	172.2	398.3
	SD	123	154.9	40.2	48.2	88.9	97.5	143.2	140.9	123.9	188
N (stems · ha ⁻¹)	Mean	1,082	1,280	734	906	1,473	1,478	1,298	1,222	885	998
	SD	696	638	595	525	779	670	739	562	492	540
AGB (t · ha ⁻¹)	Mean	20.8	27.0	7.5	8.9	20.5	24.5	25.8	33.7	23.2	38
	SD	12.6	13.9	5.9	6.6	10.3	10.4	13.5	12.4	11.8	15.4
G (m ² · ha ⁻¹)	Mean	95.7	138.4	28.2	33.3	87.1	112.2	125.1	183.9	110.8	235.7
	SD	74.1	90.4	25.9	30.1	55.3	61.2	84.2	81.9	74	107.8
QMD (cm)	Mean	16.3	16.8	11.9	10.9	13.8	15.0	16.6	19.6	19.1	23.3
	SD	5.6	5.3	4.7	4.0	3.7	3.7	4.6	4.1	5.6	5.6
No. of plots	n	5,858	614	888	73	1,353	271	1,197	222	2,420	48

2.3 Harvester data

Harvester data were collected using four different machines between 2019 and 2021. The harvester data were collected from harvested sites that are different-sized harvest units determined by the harvesting companies. The harvested sites were final-felled forests (i.e., clear-cuts with possible retention trees) and located between latitudes 60.3 N and 64.5 N (Figure 1). Harvested sites were typically dominated by Norway spruce or Scots pine. Each harvester was equipped with a GNSS (global navigation satellite system) receiver that recorded a geographical location when a tree was felled. Three of the harvesters were capable of determining the position of the boom tip with sensors recording crane length and orientation, whereas one harvester only

registered machine positions. The geographical locations of trees that were based on machine positions were stripe-patterned on the site and were post-processed by distributing the XY positions by adding a random error of 8 m to both X and Y coordinates (Räty et al., 2021b). The positioning errors associated with the harvested trees are assumed to vary between 5–20 m.

The harvested sites were overlaid with the stand-like segments of the forest resource map SR16 (Astrup et al., 2019; Hauglin et al., 2021). Since the harvested sites did not always follow the SR16 segmentation, we first delineated the harvested sites using an alpha shape approach ($\alpha = 25$) that created segments based on the XY positions of the harvested trees. Finally, each SR16 segment was cropped with the corresponding alpha shape to establish a *harvested segment*. More information on the generation of harvested segments can be found in Räty et al. (2021b). In total, 277 harvested segments were further split into 1,024 m² units (*harvested grid cells*) that were used as modeling units. The grid cell size was selected based on prior knowledge on the effect of modeling unit size when using harvester data. Saukkola et al. (2019) suggested that expanding the grid cell size mitigates the negative effects inherited from the uncertain XY positioning of harvested trees. We accepted all grid cells that had at minimum 80 % of area inside the boundaries of harvested segments. A total of 1,608 harvested grid cells containing 118,699 harvested trees were utilized in this study. 84, 14 and 2 % of the harvested grid cells were dominated by Norway spruce, Scots pine, and deciduous species, respectively.

The harvester data were saved in the Standard for Forest machine Data and communication (StandForD2010) format (Arlinger et al., 2012). The harvesters registered diameter measurements along stem, log product lengths and log product volumes (Nordström and Hemmingsson, 2018), but they did not register the timber volume associated with treetops. The following steps were taken to overcome this limitation (Hauglin et al., 2018; Räty et al., 2021b):

tree height was predicted using species-specific height-diameter curves (Blingsmo, 1985; Eide, 1954; Strand, 1967) that were iteratively calibrated according to harvester-based diameter measurements along the stem. The harvester-based diameter measurements were also used to estimate DBH for each tree. The estimated DBH and predicted tree height were used as input parameters in species-specific volume functions (Breidenbach et al., 2020a) to obtain total volume for each harvested tree.

AGB was predicted for each tree with species-specific biomass functions used in the Norwegian NFI (Breidenbach et al., 2020a). Harvester-based DBH estimate and predicted tree height were used as input parameters in the models.

The forest attributes V, HL, N, AGB, G, and QMD were calculated at the level of harvested grid cells. Predicted tree heights were used for HL, whereas G and QMD were calculated based on harvester-based DBH estimates. Table 2 shows means and standard deviations associated with the forest attributes in the harvested grid cells. Figure 2 shows the DBH distribution of all harvested trees in the harvested grid cells.

Table 2. Means and standard deviations (SDs) of forest attributes in the harvested grid cells (n = 1,608).

	Mean	Standard deviation
V (m ³ · ha ⁻¹)	210.4	114.9
HL (m)	16.8	2.9
N (stems · ha ⁻¹)	760	398
AGB (t · ha ⁻¹)	26.0	11.3
G (m ² · ha ⁻¹)	134.5	67.6
QMD (cm)	21.5	3.9

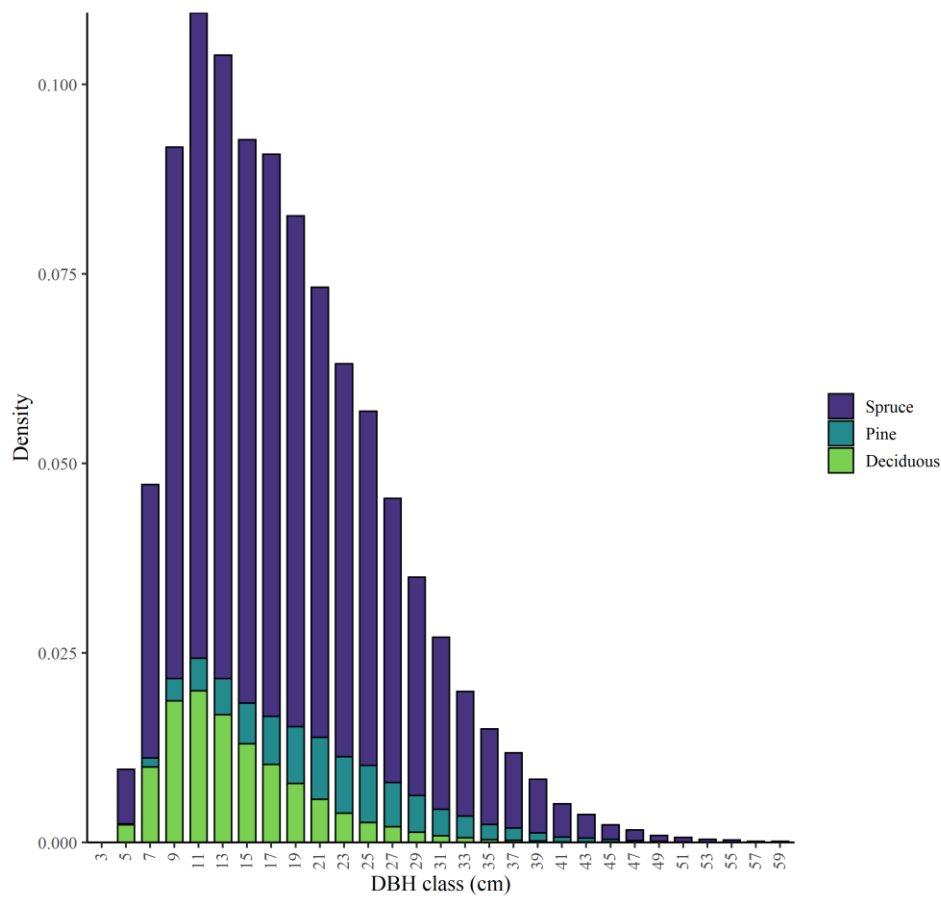


Figure 2. Diameter at breast height (DBH) distribution of trees in the harvester data.

2.4 Airborne laser scanning data

ALS data were collected in several flight campaigns between 2010 and 2018 (Hauglin et al., 2021). The flight parameters differed among the ALS campaigns and the resulting mean point densities varied between 2–5 points per square meter. A digital terrain model (DTM, 1 m × 1 m) was created using the last returns of the ALS data (Kartverket, 2019). The DTM was subtracted from the orthometric elevation measurements of the ALS data to obtain normalized height measurements. According to previous knowledge on the modeling of the forest attributes in the study area, we only calculated metrics based on the first echoes. The normalized ALS data were overlaid with the NFI plots and harvested grid cells in order to calculate height mean, variance, and percentiles (10th, 25th, 50th, 75th, and 95th). We also calculated a density metric (d2), which indicates the proportion of echoes above 2 m. The calculated ALS metrics are given in Table 3.

Table 3. Metrics calculated from the height measurements of airborne laser scanning (ALS) data.

Metric	Description
hmean	Mean of ALS height measurements.
hvar	Variance of ALS height measurements.
h10, ..., h95	Percentile calculated from ALS height measurements. Percentiles: 10th, 25th, 50th, 70th and 95th.
d2	Proportion of ALS height measurements above 2 m threshold

2.5 Study workflow

This study consisted of four steps (Figure 3). (1) Harvester models were fitted using harvester and ALS data. (2) The models were used to predict forest attributes at the NFI data. (3) The predictions were evaluated per maturity class and dominant tree species in all forest plots (ALL)

and per maturity class in potentially managed forests (PROD). (4) Evaluations large-area MA estimation and systematic errors of synthetic estimates were carried out in the 8.7 Mha study area.

Each step of the workflow is explained in detail in Sections 2.6 and 2.7.

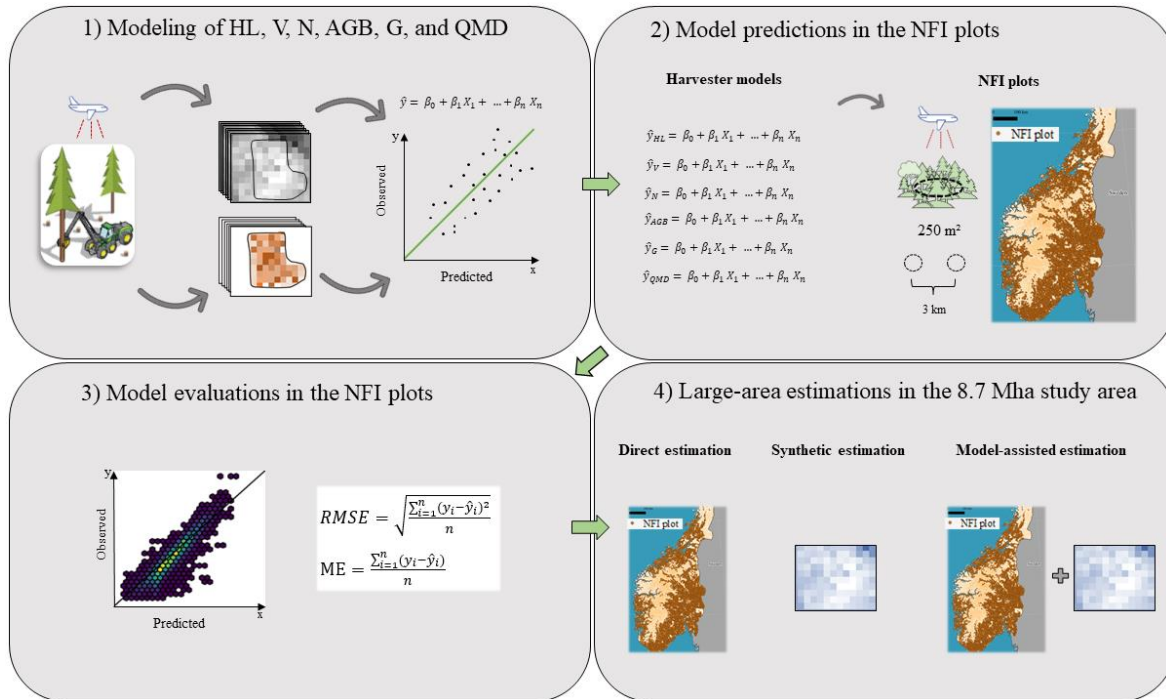


Figure 3. Study workflow. NFI – National forest inventory, HL – Lorey’s height, V – volume, N – stem frequency, AGB –above-ground biomass, G – basal area, QMD – quadratic mean diameter, RMSE – root-mean-squared error, ME – mean error.

2.6 Modeling of forest attributes

2.6.1 Harvester models

Coefficients of linear regression models were estimated using ordinary least squares (OLS) technique. The OLS models have performed well compared with well-known machine learning approaches, such as k nearest neighbor and Random Forests (Cosenza et al., 2021). In this study, the OLS model’s capability to extrapolate beyond the training data is a desired characteristic in

the model application phase. The training data consisted of the harvested grid cells with harvester-collected tree measurements and ALS metrics.

We manually selected the predictor variables based on subject-matter theory and our prior knowledge on the forest attribute modeling in the study area. We also took into account the resolution mismatch between the training and test data, which is a possible source of systematic errors in the large-area applications that aim to yield unbiased estimates (Packalen et al., 2019). In order to minimize the scaling effect, we preferred predictor variables that have resolution invariant means (e.g. height mean and proportions of echoes above a fixed threshold) and did not use nonlinear transformation on response variables. It must be noted that the theory of resolution invariant means holds in conditions with constant number of echoes per plot and when the forest attribute is additive in nature. Some forest attributes, namely LH and QMD in our study, are only additive under the constraint of a constant number of trees per area unit.

The time lag between the collection of ALS data and harvester data was on average of 6 growing seasons and ranged between 2 and 9 growing seasons. This could cause systematic errors when harvester models are applied in independent data. The time lag between the acquisition of ALS data and field measurements was therefore incorporated as a predictor variable ($time_{diff}$) in the models as also described by (Hauglin et al., 2021). The $time_{diff}$ predictor variable accounts for the mismatch between the ALS and field data acquisition and denotes the number of growing seasons between the ALS data acquisition and field measurements. The expected effect of the $time_{diff}$ variable in the forest attribute models, except the model for N, is to obtain a positive coefficient estimate which indicates that the predicted values increase when $time_{diff}$ increases. We did not employ the $time_{diff}$ variable if the interpretation of the coefficient estimate was not reasonable according to subject-matter knowledge.

2.6.2 Performance assessments

Predictive performances of the forest attribute models were evaluated using predicted- R^2 (Eq. 1), root-mean-square error (RMSE, Eq. 2), and mean error (ME, Eq. 3).

$$\text{predicted-}R^2 = 1 - \frac{\sum_{i=1}^n (y_i - \hat{y}_i)^2}{\sum_{i=1}^n (y_i - \bar{y})^2} \quad (1)$$

where y_i and \hat{y}_i are observed and predicted values in unit i . The number of units in data is denoted by n . For simplicity, we will refer to the predicted- R^2 as R^2 .

$$\text{RMSE} = \sqrt{\frac{\sum_{i=1}^n (y_i - \hat{y}_i)^2}{n}} \quad (2)$$

$$\text{ME} = \frac{\sum_{i=1}^n (y_i - \hat{y}_i)}{n} \quad (3)$$

The R^2 , RMSE and ME values were calculated both in the training data and test data. We use the subscript “TRAIN” (e.g. $\text{RMSE}_{\text{TRAIN}}$) to indicate that training data were used in the model evaluation. Whenever necessary, we also use subscripts ALL and PROD for performance measures to distinguish test data. The relative RMSE (RMSE%) and ME (ME%) were calculated by dividing absolute value by the observed mean of forest attribute. The predictive performances of the models were also visually evaluated by observed vs predicted figures in the training and test data.

2.7 Large-area estimation of forest attributes

2.7.1 Direct estimation

Direct estimation refers to the case in which forest attribute estimates and their variances are calculated based on the NFI data. Our interest was on the forested land, which means that we calculated the estimates as a ratio of forest attribute and forest land area estimates (Mandallaz,

2008, p. 63). The NFI plots that had plot center in forest were considered as forest land plots. In case of non-additive attribute (HL), forest land refers to forest land with measured trees.

The direct estimator for mean forest attribute $\hat{\mu}$ per forest land is

$$\hat{\mu} = \frac{\sum_{j \in S} y_j I_j}{\sum_{j \in S} I_j} \quad (4)$$

where I_j is an indicator variable that takes a value 1 when NFI plot j is on forest land and 0 on non-forest land. S refers to the probability sample in the study area.

There exists no design-unbiased variance estimator available for systematic sampling design. However, simulation studies and empirical analysis have shown that a variance estimator assuming simple random sampling (SRS) provides acceptable variance estimates (always conservative) also under systematic sampling designs in the case of low sampling proportions that are typical for NFIs (Magnussen et al., 2020; Rätty et al., 2021a). A variance estimator for $\hat{\mu}$ assuming SRS (Mandallaz, 2008, p. 63) is

$$\widehat{var}(\hat{\mu}) = \frac{1}{n_S \left(\frac{\sum_{j \in S} I_j}{n_S} \right)^2} \frac{1}{n_S - 1} \sum_{j \in S} (z_j)^2 \quad (5)$$

where $z_j = (y_j - \hat{\mu})I_j$ and n_S refers to the number of NFI plots in the sample S .

The standard error (SE) of an estimate is

$$SE(\hat{\mu}) = \sqrt{\widehat{var}(\hat{\mu})} \quad (6)$$

We used $2 \times SE$ to evaluate the precision of an estimate.

2.7.2 Model-assisted estimation

The MA estimator utilizes predictive modeling and a probability sample in the estimation of population parameters. If the predictive model can explain the variance of the forest attributes well enough, MA estimates are more precise than direct estimates.

The MA estimator includes two components: (1) synthetic estimate $\hat{\mu}_{syn}$ and (2) an estimate of a correction factor ($\hat{\mu}_{cor}$). The $\hat{\mu}_{cor}$ component is used to correct the systematic error associated with the model predictions.

The MA estimator is

$$\hat{\mu}_{MA} = \hat{\mu}_{syn} + \hat{\mu}_{cor} \quad (7)$$

where $\hat{\mu}_{cor} = \frac{\sum_{j \in S} e_j I_j}{\sum_{j \in S} I_j}$ in which e_j refers to residual ($y_j - \hat{y}_j$) in NFI plot j (Breidenbach et al., 2021b).

The variances of the MA estimates were calculated using the SRS estimator (Eq. 4) with $z_j = (e_j - \bar{e})I_j$ where \bar{e} is the mean of model residuals observed in the NFI plots of interest. Note that the map-based estimate $\hat{\mu}_{syn}$ is not needed to evaluate variance estimates. We predicted the forest attributes for the NFI plots using the harvester models to obtain e_j . Observed forest land classification was used in the MA estimation, which means that we assumed an error-free classifications of forest land and non-forest land in the study area.

2.7.3 Evaluating efficiencies of estimators

The efficiencies of the estimators were evaluated using SE, and relative efficiency (RE). The RE allows a comparison of the direct and MA estimators and is given by

$$RE = \frac{v\hat{a}r(\hat{\mu})}{v\hat{a}r(\hat{\mu}_{MA})} \quad (8)$$

The RE values allow a straightforward comparison between the efficiencies of the estimators, and an RE value larger than 1 indicates that MA estimator is more efficient than direct estimator. Assuming SRS, the number of sample plots required to achieve the same variance as the MA estimate can be calculated by means of RE. Given that the MA estimation determines the desired variance, the similar variance can be achieved via SRS by increasing n_S (the number of sample plots) by $n_S \times RE$.

3 Results

3.1 Predictive performances of the harvester models in the training data

Figure 4 shows observed versus predicted values associated with the model predictions in the training data. The model coefficients, $RMSE\%_{TRAIN}$, and R^2 values associated with the harvester models are given in Table 4. The $RMSE\%_{TRAIN}$ values associated with the model predictions were 6.8, 30.3, and 39.0 % for HL, V, and N, respectively. The R^2 value was largest for HL ($R^2=0.85$) followed by V ($R^2=0.69$) and N ($R^2=0.44$). The estimated model coefficients and their standard errors are in Table 4. The results associated with AGB, G, and QMD are shown in the Appendix to simplify the presentation and because they were comparable to the results for HL, V and N.

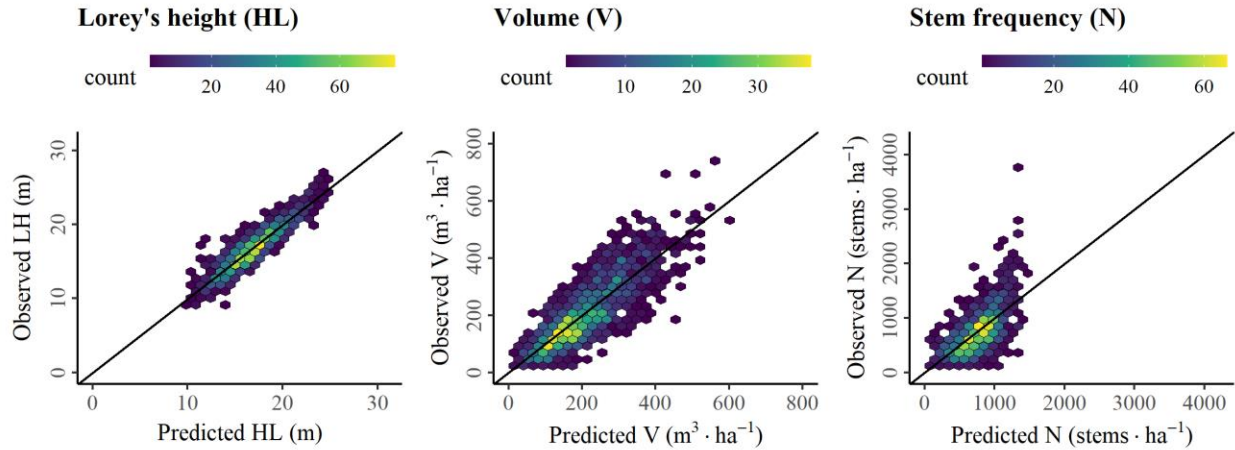


Figure 4. Observed versus predicted values associated with the harvester models in the training data.

Table 4. Estimated coefficients, standard errors (SEs) of coefficients, p-values (p), relative root-mean-square errors (RMSE%s) and coefficients of determination (R^2 s) associated with the forest attribute models fit using harvester and airborne laser scanning data.

<i>Predictors</i>	Lorey's height			Volume			Stem frequency		
	<i>Estimates</i>	<i>SE</i>	<i>p</i>	<i>Estimates</i>	<i>SE</i>	<i>p</i>	<i>Estimates</i>	<i>SE</i>	<i>p</i>
(Intercept)	3.77	0.17	<0.001	-76.09	8.28	<0.001	-497.48	36.17	<0.001
h95	0.77	0.01	<0.001						
hmean	-0.04	0.02	0.016	33.84	1.00	<0.001	-48.10	4.46	<0.001
time _{diff}	0.19	0.01	<0.001	9.23	0.67	<0.001			
d2				-6.14	18.95	0.746	2426.77	84.97	<0.001
RMSE% _{TRAIN}	6.75			30.30			39.03		
R^2	0.85			0.69			0.44		

3.2 Predictive performance of the harvester models in the test data

Figure 5 shows the observed versus predicted values for the plots of the ALL data dominated by spruce, pine, and deciduous species. The harvester models performed better in coniferous-

dominated than deciduous-dominated forests. The HL and V predictions associated with deciduous-dominated plots were considerably overpredicted. For all attributes (HL, V, and N), the smallest RMSE% values were reported in spruce dominated forests. The harvester model for N tended to yield underpredictions regardless of dominant tree species, while the most considerable underpredictions were observed in plots with large stem frequency, i.e. typically young forests (see also Figure 6).

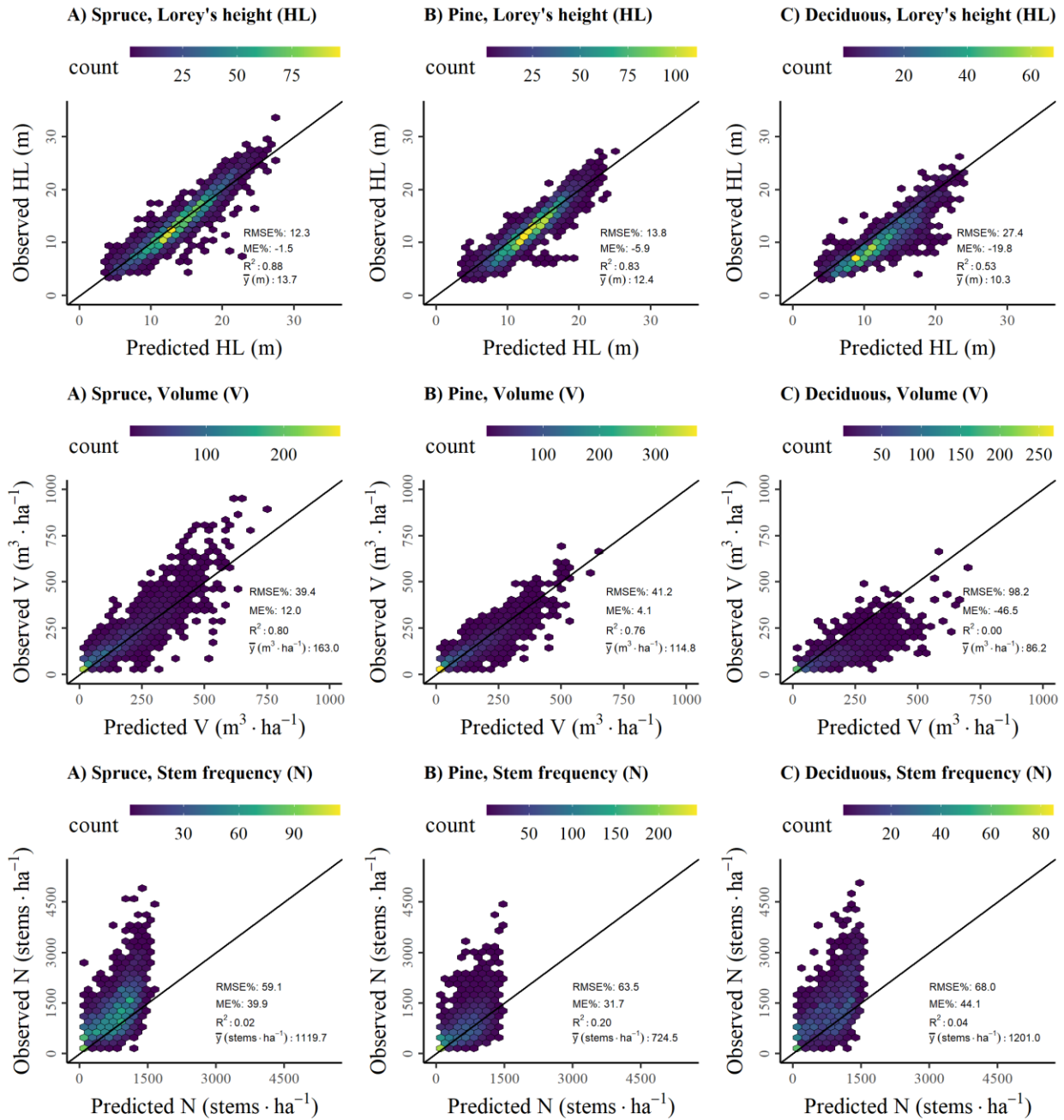


Figure 5. Observed versus predicted values by dominant tree species (Spruce: Norway spruce, Pine: Scots pine, Deciduous: Deciduous species) in the ALL test data.

Figure 6 shows the RMSE% and ME% values associated with the predictions in the ALL and PROD data by maturity classes M2, ..., M5 (and all maturity classes M2–M5). The RMSE%_{PROD} values were always smaller than the RMSE%_{ALL} values, which indicates that the harvester

models performed better in PROD than in ALL data. The harvester models resulted in the smallest $RMSE\%_{PROD}$ values in maturity classes M4 and M5.

The ME% values associated with V were close to zero in the maturity classes M3, M4, and M5 with the ALL data. The ME% value was also close to zero (-0.8 %) when all maturity classes M2–M5 were considered. The ME% values associated with N and V models were considerable ($|ME\%| > 24\%$) in the maturity class M2 indicating severe systematic prediction errors. The results associated with the harvester model of N indicated that the smallest systematic errors were in old forests (M5), although the ME% values associated with N were considerable regardless of maturity class and test data.

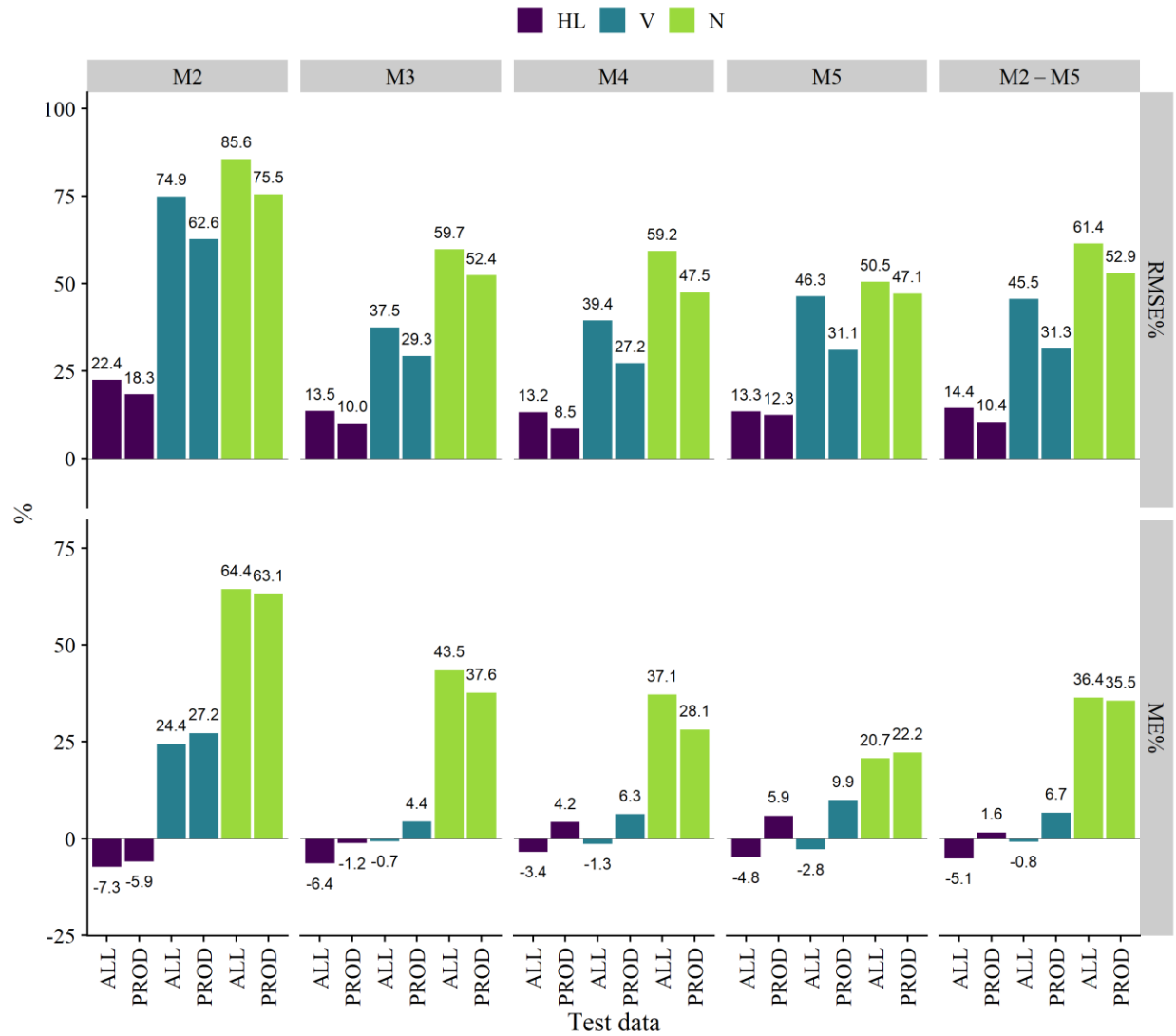


Figure 6. Relative root-mean-square errors (RMSE%) and mean errors (ME%) associated with the forest attribute predictions by maturity classes in the ALL and PROD test data. HL – Lorey’s height, V – volume, N – stem frequency. Please refer to Section 2.2 for the maturity classification.

3.1 Large-area estimation of forest attributes

Characteristics associated with the large-area estimations of the forest attributes for forested land (includes all maturity classes M1–M5) are presented in Table 5. Non-zero $\hat{\mu}_{cor}$ values indicate that the application of the harvester models for the large-area synthetic estimation of forest attributes would result in systematic estimation errors given that the estimates were not corrected

by means of a probability sample of field plots. The largest systematic estimation errors were observed for N ($\hat{\mu}_{cor} = 39.0$ % of the direct estimate). The smallest systematic error of the synthetic estimate was observed for V ($\hat{\mu}_{cor} = 0.8$ % of the direct estimate).

The MA estimation using the harvester models resulted in efficiency gains, compared with the direct estimation, for all forest attributes (Table 5). The smallest RE value of 1.70 was associated with N whereas the largest RE value of 6.00 was associated with the estimation of HL. In this section, we presented results concerning forest attributes HL, V, and N, whereas the results for AGB, G, and QMD are in the Appendix.

Table 5. Characteristics associated with the estimation of forest attributes for the forest land of the study area. V – volume, HL – Lorey’s height, N – stem frequency, SE – standard error.

Forest attribute	Direct estimate $\hat{\mu}$	2SE% $\hat{\mu}$ (%)	2SE% $\hat{\mu}_{MA}$ (%)	Systematic error of synthetic estimator $\hat{\mu}_{cor}$ (%)	Relative efficiency
HL (m)	12.40	0.84	0.34	-6.53	6.00
V ($m^3 \cdot ha^{-1}$)	124.09	2.16	1.14	0.82	3.58
N (stems $\cdot ha^{-1}$)	957.44	1.58	1.37	38.98	1.70

4 Discussion

Harvesters operate in forests that are considered harvest-ready from the perspective of timber production. In Norway, forests that have reached an age of 60–120 years typically fall under this definition. The decision on final felling also depends on site fertility and tree species. It is also worth noting that forests managed for timber production may have characteristics that differ from those of unmanaged forests. For example, silvicultural operations that affect the size distribution of trees, such as thinnings from below, may be carried out in productive forests. The

selection bias towards mature and productive forests associated with the training data of the harvester models manifests in larger systematic errors in young forests and deciduous-dominated forests than in older coniferous forests. Deciduous species are currently rarely used for commercial timber production purposes in Norway, and deciduous trees were therefore rare in our harvester dataset. Systematic errors were also reported for the large-area synthetic estimates. However, systematic errors can also by chance balance out as was the case for timber volume in our study. Timber volume had a tendency to be underpredicted in spruce forests and overpredicted in deciduous forests. In total over the whole study area, this resulted in a systematic error close to 1 %.

Non-harvested trees, e.g. retention trees, are also a possible source of systematic estimation error, since they are usually left out of final fellings due to ecological reasons. Currently, the harvesters are not capable of recording the retention trees, and therefore we were not able to observe the possible mismatches between the harvester and ALS data. Close-range remote sensing solutions, that are capable of measuring tree-level attributes rapidly and accurately in forest stands (Ahola et al., 2021), could open possibilities to also keep track on trees left out of harvest operations.

Studies using harvester data as the reference for ALS-based forest inventories are still rare. The collection of harvester data has, nonetheless, already begun to mature towards operational standard in Sweden (Söderberg et al., 2021). In the prediction of forest attributes, Söderberg et al. (2021) and Maltamo et al. (2019) reported smaller RMSEs (10–15 % and 9–15 %) for merchantable timber volume compared with our results associated with timber volume, because their level of validation was the stand-level, while we validated our results at the plot level. The reduction of uncertainty is a known property when aggregating estimates from finer into coarser scales (Kotivuori et al., 2021). Saukkola et al. (2019) predicted timber volume at the stand-level

and reported, depending on modeling unit sizes, RMSEs of 26–31 % that are larger than our RMSEs reported at the plot-level for older production forests. They used a limited set of harvester data in the training of the model that may have negatively affected the stand-level accuracy they reported. Hauglin et al. (2018) reported RMSEs of 19–22 % and 32–56 % for timber volume in high-productive and low-productive forests at the level of 400 m² grid cells, respectively. Those uncertainties are approximately in line with ours for timber volume in older managed forest (RMSEs of 27 and 31 %). Noordermeer et al. (2022) estimated timber volume at the harvested site (i.e., a cluster of adjacent stands) level with an RMSE% of 9–17 % depending on the modeling unit size and simulated tree positioning errors. For 400 m² grid cells, they reported cross-validated RMSEs of 18–22 % depending on simulated tree positioning errors, which are smaller than our RMSE in older production forest (RMSE of 27 %). A possible reason for this is that the data used by Noordermeer et al. (2022) came from fewer harvested sites and were less variable compared with our test data that comprised independent NFI plots.

Söderberg et al. (2021) reported systematic errors for volume of 2–4 % although the predictive models were validated in harvest-ready forests. Similarly, Hauglin et al. (2018) reported systematic prediction errors of 4–11 % for volume in a highly productive forest. We found systematic prediction errors of 6.6 and 9.9 % for volume in older productive forests, whereas the systematic errors were -1.3 and -2.8 % in all older forests (M4 and M5). The close to zero systematic prediction errors associated with all older forests can be largely explained by the volume model's tendency to overpredict in deciduous-dominated forests. The comparison of these studies indicates that systematic errors associated with harvester model predictions are difficult to avoid even if forests to be mapped resemble harvest-ready stands.

The efficiency of an estimator can be evaluated using the RE (relative efficiency). In our case, the RE can be interpreted as the number of additional field sample plots that would be required to obtain the same precision in direct (field-data based) estimation as in MA estimation that takes advantage of the harvester model and ALS data. The RE of 1.70 for stem number thus suggests that 70 % more field data would be required to achieve the same precision without using harvester and ALS data. There exist few comparable studies that have carried out MA estimations using field and ALS data. Rätty et al. (2021a) reported an RE value of 2.11 for stem frequency with the MA estimator that used a model constructed for the prediction of DBH distributions using Norwegian NFI and ALS data. Rätty et al. (2021a) also reported of much smaller systematic error that was 1.4 % compared with 39.0 % in our study. We re-analyzed a dataset by Hauglin et al. (2021) used NFI and ALS data for large-scale mapping of forest attributes in Norway. We calculated REs of MA estimators of HL, V, AGB, and G (for details see Appendix A6). The data of Hauglin et al. (2021) resulted in considerable larger RE values (7.85 for HL, 6.21 for V, 5.72 for AGB, and 5.10 for G) compared with the MA estimations using harvester models and ALS data (6.00 for HL, 3.58 for V, 3.27 for AGB, and 3.51 for G). These findings show that the combination of field plots and ALS data can be more advantageous than the combination of harvester and ALS data. However, the harvester data which were used here and in other studies so far are rather limited in terms of the number observations, areal coverage or positioning accuracy. Considerable improvements may therefore be expected in the future, if the availability of harvester data improves.

Inaccuracy associated with the geographic positions of trees limits the use of harvester data, and the positioning errors of trees are also a potential source of uncertainty in modeling and mapping (Noordermeer et al., 2022). In order to minimize the effect of positioning errors, we utilized

modeling units that are up to four times larger than the area covered by the NFI plots. According to Saukkola et al. (2019), the increase in the size of modeling unit from 254 m² to 761 m² or larger moderates the uncertainty associated with geographic positions of trees. Noordermeer et al. (2022) also showed that prediction errors due to positioning errors of trees can be considerably reduced by increasing the size of modeling unit from 100 m² to 400 m². The positioning accuracy of harvested trees can be improved by modern positioning technology, and it has been shown that sub-meter accuracy can be achieved with a differential GNSS system coupled with harvester boom sensors (Hauglin et al., 2017; Noordermeer et al., 2021). To the best of our knowledge, sub-meter positioning systems are so far not used operationally. Therefore, current operational applications must cope with positioning errors, for example, by increasing the size of modeling units.

The size of a harvested grid cell in our study was four times larger than the size of the NFI plots used for model testing. This resolution mismatch may account for prediction errors when the models are applied in the test data. Packalen et al. (2019) showed that the prediction errors tended to decrease when training plots were larger compared to test plots. They also reported that resolution mismatch caused systematic errors, but they also concluded that the resolution dependency had a minor effect in most real-world use cases. We minimized the effect of resolution mismatch by preferring predictor variables that are resolution invariant, but it was not always reasonable in terms of predictive performance. For example, the predictive performance of the HL model would have been considerably degraded after omitting the non-resolution-invariant variable h95 from the model.

This study shows that harvester data constitute a potential data source for the creation of forest attribute maps. However, the risk of systematic errors exists, and the magnitude of systematic

error may be challenging to ascertain based on the harvester data. The risk of systematic errors in the synthetic estimation of forest attributes can be eliminated using MA estimation given that a comprehensive probability sample is available in the area of interest. Even maps with large systematic errors can then generate considerable efficiency gains.

Conclusions

We draw the following conclusions from this study:

- 1) The selection bias of harvesters towards harvest-ready sites negatively affects the predictive performance of harvester-based models in the mapping of forest attributes.
- 2) Synthetic (pixel-counting) estimates resulting from forest attribute maps created using harvester and airborne laser scanning data are likely to contain systematic errors. Systematic errors can, however, by chance cancel each other out in large-area estimation.
- 3) Systematic errors can be corrected using a model-assisted estimator if a comprehensive probability sample is available.
- 4) Model-assisted estimators, despite utilizing synthetic estimates with large systematic errors, can result in considerable efficiency gains compared with field data-based direct estimators. This can be used for reducing the field sampling intensity without increasing uncertainties or for decreasing uncertainties without increasing the field sampling intensity.

Acknowledgements

This study was supported by the Norwegian research council through the PRECISION project – Precision forestry for improved resource use and reduced wood decay in Norwegian Forests (NFR 281140). We acknowledge Simon Berg for technical support with the harvester data.

References

- Ahola, J.M., Heikkilä, T., Raitila, J., Sipola, T., Tenhunen, J., 2021. Estimation of breast height diameter and trunk curvature with linear and single-photon LiDARs. *Annals of Forest Science* 78, 1–13. <https://doi.org/10.1007/s13595-021-01100-0>
- Arlinger, J., Nordström, M., Möller, J., 2012. StandForD 2010: Modern kommunikation med skogsmaskiner.
- Asner, G.P., Mascaro, J., Muller-Landau, H.C., Vieilledent, G., Vaudry, R., Rasamoelina, M., Hall, J.S., van Breugel, M., 2012. A universal airborne LiDAR approach for tropical forest carbon mapping. *Oecologia* 168, 1147–1160. <https://doi.org/10.1007/s00442-011-2165-z>
- Astrup, R., Rahlf, J., Bjørkelo, K., Debella-Gilo, M., Gjertsen, A.-K., Breidenbach, J., 2019. Forest information at multiple scales: development, evaluation and application of the Norwegian forest resources map SR16. *Scandinavian Journal of Forest Research* 34, 484–496. <https://doi.org/10.1080/02827581.2019.1588989>
- Blingsmo, K., 1985. Avsmalingsfunksjoner og -tabeller for bjørk. Rapport fra Norsk institutt for skogforskning 10, 35.
- Bollandsås, O.M., Maltamo, M., Gobakken, T., Lien, V., Næssset, E., 2013. Prediction of Timber Quality Parameters of Forest Stands by Means of Small Footprint Airborne Laser Scanner Data. *International Journal of Forest Engineering*.
- Breidenbach, J., Ellison, D., Petersson, H., Korhonen, K.T., Henttonen, H.M., Wallerman, J., Fridman, J., Gobakken, T., Astrup, R., Næssset, E., 2021a. Harvested area did not increase abruptly – How advancements in satellite-based mapping led to erroneous conclusions. <https://doi.org/10.5281/zenodo.4972189>
- Breidenbach, J., Granhus, A., Hysten, G., Eriksen, R., Astrup, R., 2020a. A century of National Forest Inventory in Norway – informing past, present, and future decisions. *Forest Ecosystems* 7, 46. <https://doi.org/10.1186/s40663-020-00261-0>
- Breidenbach, J., Ivanovs, J., Kangas, A., Nord-Larsen, T., Nilsson, M., Astrup, R., 2021b. Improving living biomass C-stock loss estimates by combining optical satellite, airborne laser scanning, and NFI data. *Can. J. For. Res.* 51, 1472–1485. <https://doi.org/10.1139/cjfr-2020-0518>

Breidenbach, J., Waser, L.T., Debella-Gilo, M., Schumacher, J., Rahlf, J., Hauglin, M., Puliti, S., Astrup, R., 2020b. National mapping and estimation of forest area by dominant tree species using Sentinel-2 data. *Can. J. For. Res.* <https://doi.org/10.1139/cjfr-2020-0170>

Ceccherini, G., Duveiller, G., Grassi, G., Lemoine, G., Avitabile, V., Pilli, R., Cescatti, A., 2020. Abrupt increase in harvested forest area over Europe after 2015. *Nature* 583, 72–77. <https://doi.org/10.1038/s41586-020-2438-y>

Cosenza, D.N., Korhonen, L., Maltamo, M., Packalen, P., Strunk, J.L., Næsset, E., Gobakken, T., Soares, P., Tomé, M., 2021. Comparison of linear regression, k-nearest neighbour and random forest methods in airborne laser-scanning-based prediction of growing stock. *Forestry: An International Journal of Forest Research* 94, 311–323. <https://doi.org/10.1093/forestry/cpaa034>

Eide, E., 1954. Avsmalingstabell for granskog. Utvidet og revidert 1954. *Meddr. norske SkogforsVes* 63.

Fedrowitz, K., Koricheva, J., Baker, S.C., Lindenmayer, D.B., Palik, B., Rosenvald, R., Beese, W., Franklin, J.F., Kouki, J., Macdonald, E., Messier, C., Sverdrup-Thygeson, A., Gustafsson, L., 2014. REVIEW: Can retention forestry help conserve biodiversity? A meta-analysis. *Journal of Applied Ecology* 51, 1669–1679. <https://doi.org/10.1111/1365-2664.12289>

Hauglin, M., Hansen, E., Sørngård, E., Næsset, E., Gobakken, T., 2018. Utilizing accurately positioned harvester data: modelling forest volume with airborne laser scanning. *Canadian Journal of Forest Research.* <https://doi.org/10.1139/cjfr-2017-0467>

Hauglin, M., Hansen, E.H., Næsset, E., Busterud, B.E., Gjevestad, J.G.O., Gobakken, T., 2017. Accurate single-tree positions from a harvester: a test of two global satellite-based positioning systems. *Scandinavian Journal of Forest Research* 32, 774–781. <https://doi.org/10.1080/02827581.2017.1296967>

Hauglin, M., Rahlf, J., Schumacher, J., Astrup, R., Breidenbach, J., 2021. Large scale mapping of forest attributes using heterogeneous sets of airborne laser scanning and National Forest Inventory data. *Forest Ecosystems* 8, 65. <https://doi.org/10.1186/s40663-021-00338-4>

Kangas, A., Maltamo, M. (Eds.), 2006. *Forest inventory: methodology and applications, Managing forest ecosystems.* Springer, Dordrecht.

Karjalainen, T., Packalen, P., Rätty, J., Maltamo, M., 2019. Predicting factual sawlog volumes in Scots pine dominated forests using airborne laser scanning data. *Silva Fennica* 53. <https://doi.org/10.14214/sf.10183>

Kartverket, 2019. Høydedata og terrengmodeller for landområdene.

Kemmerer, J., Labelle, E.R., 2020. Using harvester data from on-board computers: a review of key findings, opportunities and challenges. *Eur J Forest Res.* <https://doi.org/10.1007/s10342-020-01313-4>

Kotivuori, E., Maltamo, M., Korhonen, L., Strunk, J.L., Packalen, P., 2021. Prediction error aggregation behaviour for remote sensing augmented forest inventory approaches. *Forestry: An International Journal of Forest Research* 94, 576–587. <https://doi.org/10.1093/forestry/cpab007>

- Magnussen, S., McRoberts, R.E., Breidenbach, J., Nord-Larsen, T., Ståhl, G., Fehrmann, L., Schnell, S., 2020. Comparison of estimators of variance for forest inventories with systematic sampling - results from artificial populations. *Forest Ecosystems* 7. <https://doi.org/10.1186/s40663-020-00223-6>
- Maltamo, M., Hauglin, M., Næsset, E., Gobakken, T., 2019. Estimating stand level stem diameter distribution utilizing harvester data and airborne laser scanning. *Silva Fennica* 53. <https://doi.org/10.14214/sf.10075>
- Maltamo, M., Packalen, P., 2014. Species-Specific Management Inventory in Finland, in: Maltamo, M., Næsset, E., Vauhkonen, J. (Eds.), *Forestry Applications of Airborne Laser Scanning: Concepts and Case Studies, Managing Forest Ecosystems*. Springer Netherlands, Dordrecht, pp. 241–252. https://doi.org/10.1007/978-94-017-8663-8_12
- Maltamo, M., Packalen, P., Kangas, A., 2021. From comprehensive field inventories to remotely sensed wall-to-wall stand attribute data — a brief history of management inventories in the Nordic countries. *Can. J. For. Res.* 51, 257–266. <https://doi.org/10.1139/cjfr-2020-0322>
- Mandallaz, D., 2008. *Sampling techniques for forest inventories*. Chapman & Hall/CRC.
- McRoberts, R.E., Chen, Q., Walters, B.F., 2017. Multivariate inference for forest inventories using auxiliary airborne laser scanning data. *Forest Ecology and Management* 401, 295–303. <https://doi.org/10.1016/j.foreco.2017.07.017>
- Næsset, E., 2014. Area-Based Inventory in Norway – From Innovation to an Operational Reality, in: Maltamo, M., Næsset, E., Vauhkonen, J. (Eds.), *Forestry Applications of Airborne Laser Scanning: Concepts and Case Studies, Managing Forest Ecosystems*. Springer Netherlands, Dordrecht, pp. 215–240. https://doi.org/10.1007/978-94-017-8663-8_11
- Næsset, E., 1997. Estimating timber volume of forest stands using airborne laser scanner data. *Remote Sensing of Environment* 61, 246–253. [https://doi.org/10.1016/S0034-4257\(97\)00041-2](https://doi.org/10.1016/S0034-4257(97)00041-2)
- Nilsson, M., Nordkvist, K., Jonzén, J., Lindgren, N., Axensten, P., Wallerman, J., Egberth, M., Larsson, S., Nilsson, L., Eriksson, J., Olsson, H., 2017. A nationwide forest attribute map of Sweden predicted using airborne laser scanning data and field data from the National Forest Inventory. *Remote Sensing of Environment* 194, 447–454. <https://doi.org/10.1016/j.rse.2016.10.022>
- Noordermeer, L., Bollandsås, O.M., Ørka, H.O., Næsset, E., Gobakken, T., 2019. Comparing the accuracies of forest attributes predicted from airborne laser scanning and digital aerial photogrammetry in operational forest inventories. *Remote Sensing of Environment* 226, 26–37. <https://doi.org/10.1016/j.rse.2019.03.027>
- Noordermeer, L., Næsset, E., Gobakken, T., 2022. Effects of harvester positioning errors on merchantable timber volume predicted and estimated from airborne laser scanner data in mature Norway spruce forests. *Silva Fennica* 56, 15. <https://doi.org/10.14214/sf.10608>
- Noordermeer, L., Sørngård, E., Astrup, R., Næsset, E., Gobakken, T., 2021. Coupling a differential global navigation satellite system to a cut-to-length harvester operating system

enables precise positioning of harvested trees. *International Journal of Forest Engineering* 32, 119–127. <https://doi.org/10.1080/14942119.2021.1899686>

Nord-Larsen, T., Riis-Nielsen, T., Ottosen, M.B., 2017. Forest resource map of Denmark. Mapping of Danish forest resources using ALS from 2014 15.

Nordström, M., Hemmingsson, J., 2018. Measure up! A Skogforsk Guide to Harvester Measurement. Skogforsk, Uppsala.

Packalen, P., Strunk, J., Packalen, T., Maltamo, M., Mehtätalo, L., 2019. Resolution dependence in an area-based approach to forest inventory with airborne laser scanning. *Remote Sensing of Environment* 224, 192–201. <https://doi.org/10.1016/j.rse.2019.01.022>

Palahí, M., Valbuena, R., Senf, C., Acil, N., Pugh, T.A.M., Sadler, J., Seidl, R., Potapov, P., Gardiner, B., Hetemäki, L., Chirici, G., Francini, S., Hlásny, T., Lerink, B.J.W., Olsson, H., González Olabarria, J.R., Ascoli, D., Asikainen, A., Bauhus, J., Berndes, G., Donis, J., Fridman, J., Hanewinkel, M., Jactel, H., Lindner, M., Marchetti, M., Marušák, R., Sheil, D., Tomé, M., Trasobares, A., Verkerk, P.J., Korhonen, M., Nabuurs, G.-J., 2021. Concerns about reported harvests in European forests. *Nature* 592, E15–E17. <https://doi.org/10.1038/s41586-021-03292-x>

Rahlf, J., Hauglin, M., Astrup, R., Breidenbach, J., 2021. Timber volume estimation based on airborne laser scanning — comparing the use of national forest inventory and forest management inventory data. *Annals of Forest Science* 78, 49. <https://doi.org/10.1007/s13595-021-01061-4>

Räty, J., Astrup, R., Breidenbach, J., 2021a. Prediction and model-assisted estimation of diameter distributions using Norwegian national forest inventory and airborne laser scanning data. *Can. J. For. Res.* 51, 1521–1533. <https://doi.org/10.1139/cjfr-2020-0440>

Räty, J., Breidenbach, J., Hauglin, M., Astrup, R., 2021b. Prediction of butt rot volume in Norway spruce forest stands using harvester, remotely sensed and environmental data. *International Journal of Applied Earth Observation and Geoinformation* 105, 102624. <https://doi.org/10.1016/j.jag.2021.102624>

Ruotsalainen, R., Pukkala, T., Kangas, A., Packalen, P., 2021. Effects of errors in basal area and mean diameter on the optimality of forest management prescriptions. *Annals of Forest Science* 78, 18. <https://doi.org/10.1007/s13595-021-01037-4>

Saarela, S., Grafström, A., Ståhl, G., Kangas, A., Holopainen, M., Tuominen, S., Nordkvist, K., Hyypä, J., 2015. Model-assisted estimation of growing stock volume using different combinations of LiDAR and Landsat data as auxiliary information. *Remote Sensing of Environment* 158, 431–440. <https://doi.org/10.1016/j.rse.2014.11.020>

Saukkola, A., Melkas, T., Riekkö, K., Sirparanta, S., Peuhkurinen, J., Holopainen, M., Hyypä, J., Vastaranta, M., 2019. Predicting Forest Inventory Attributes Using Airborne Laser Scanning, Aerial Imagery, and Harvester Data. *Remote Sensing* 11, 797. <https://doi.org/10.3390/rs11070797>

Söderberg, J., Wallerman, J., Almäng, A., Möller, J.J., Willén, E., 2021. Operational prediction of forest attributes using standardised harvester data and airborne laser scanning data in Sweden.

Scandinavian Journal of Forest Research 0, 1–9.
<https://doi.org/10.1080/02827581.2021.1919751>

Strand, L., 1967. Avsmalingstabeller for furu sønnafjells. *Medd. norske SkogforsVes* 84, 431–482.

Tompalski, P., White, J.C., Coops, N.C., Wulder, M.A., 2019. Demonstrating the transferability of forest inventory attribute models derived using airborne laser scanning data. *Remote Sensing of Environment* 227, 110–124. <https://doi.org/10.1016/j.rse.2019.04.006>

Tveite, B., 1977. Bonitetskurver for gran. *Norsk Institutt for Skogforskning* 33.

Tveite, B., Braastad, H., 1981. Bonitering for gran, furu og bjørk. *Norsk Institutt for Skogforskning* 27.

Vähä-Konka, V., Maltamo, M., Pukkala, T., Kärhä, K., 2020. Evaluating the accuracy of ALS-based removal estimates against actual logging data. *Annals of Forest Science* 77, 84.
<https://doi.org/10.1007/s13595-020-00985-7>

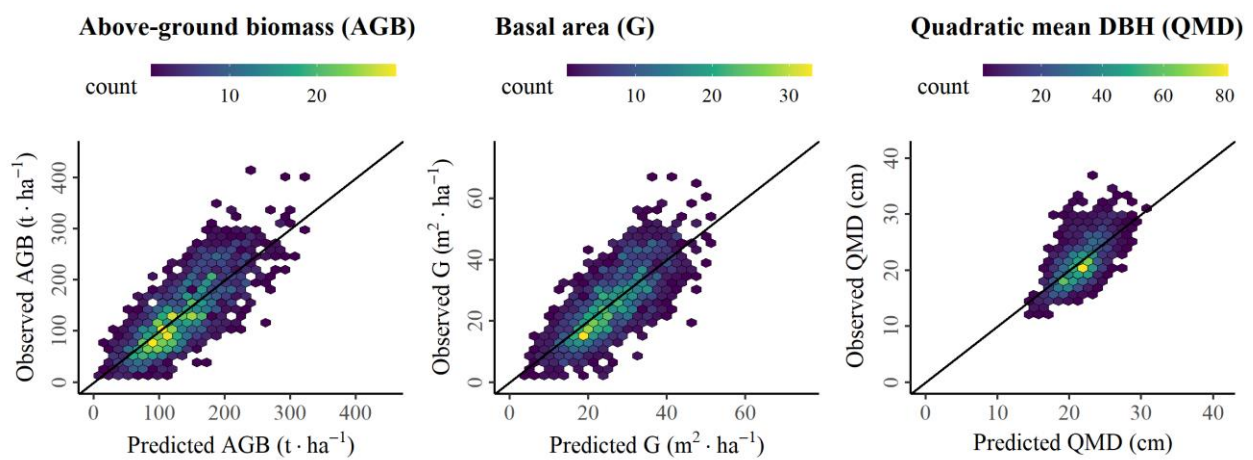
Waldner, F., Defourny, P., 2017. Where can pixel counting area estimates meet user-defined accuracy requirements? *International Journal of Applied Earth Observation and Geoinformation* 60, 1–10. <https://doi.org/10.1016/j.jag.2017.03.014>

White, J.C., Wulder, M.A., Varhola, A., Vastaranta, M., Coops, N.C., Cook, B.D., Pitt, D., Woods, M., 2013. A best practices guide for generating forest inventory attributes from airborne laser scanning data using an area-based approach. *The Forestry Chronicle* 89, 722–723.
<https://doi.org/10.5558/tfc2013-132>

1 Appendix

2

3 **Appendix A1.** Observed versus predicted values associated with the harvester models in the
4 training data. Harvester models refer to models that are fit using harvester information and
5 airborne laser scanning data.



6

7

8

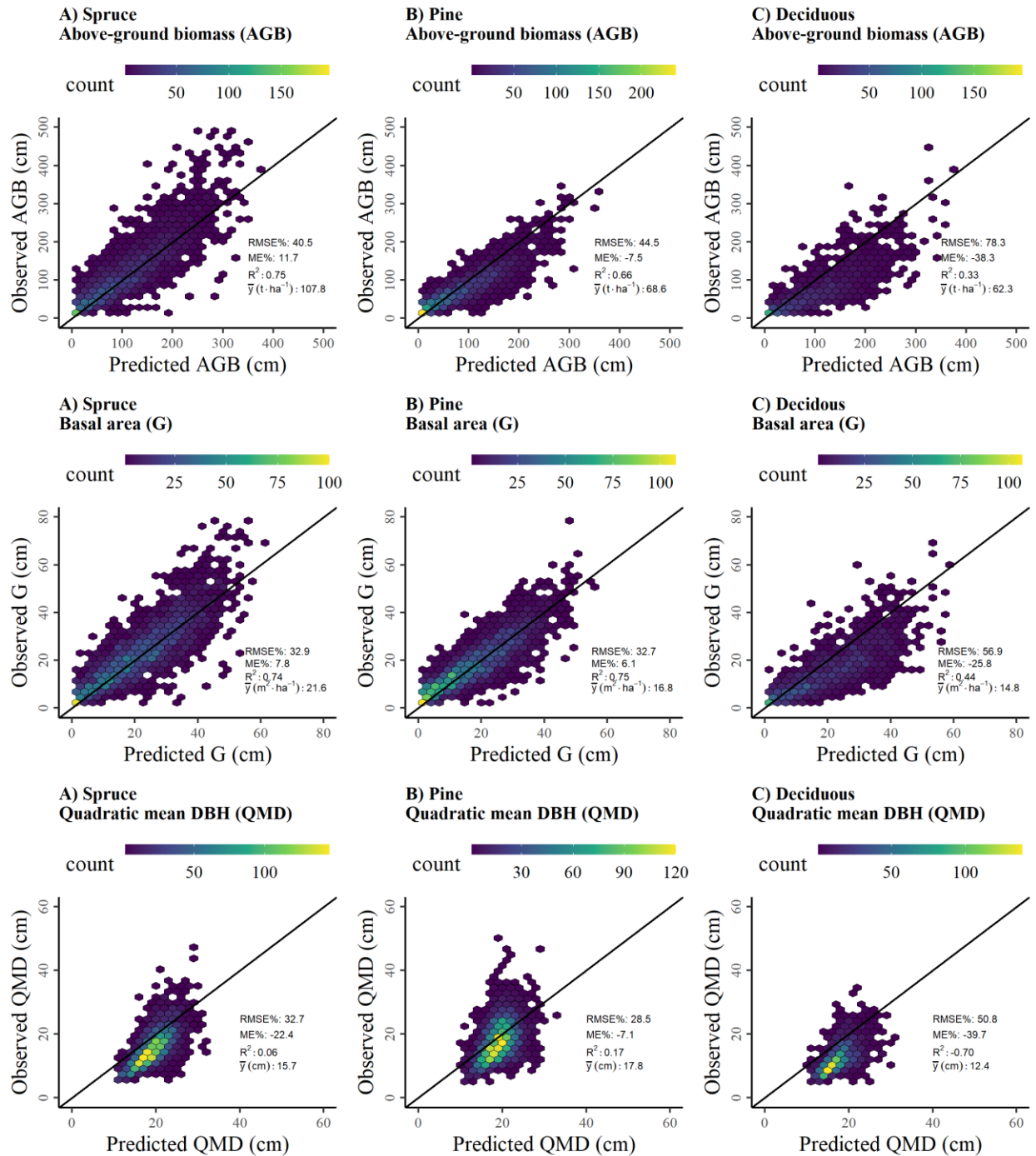
9

10

11

12 **Appendix A2.** Estimated coefficients, standard errors (SEs) of coefficients, p-values (p), relative
 13 root-mean-square errors (RMSE%) and coefficients of determination (R^2) associated with the
 14 forest attribute models fit using harvester and airborne laser scanning data.

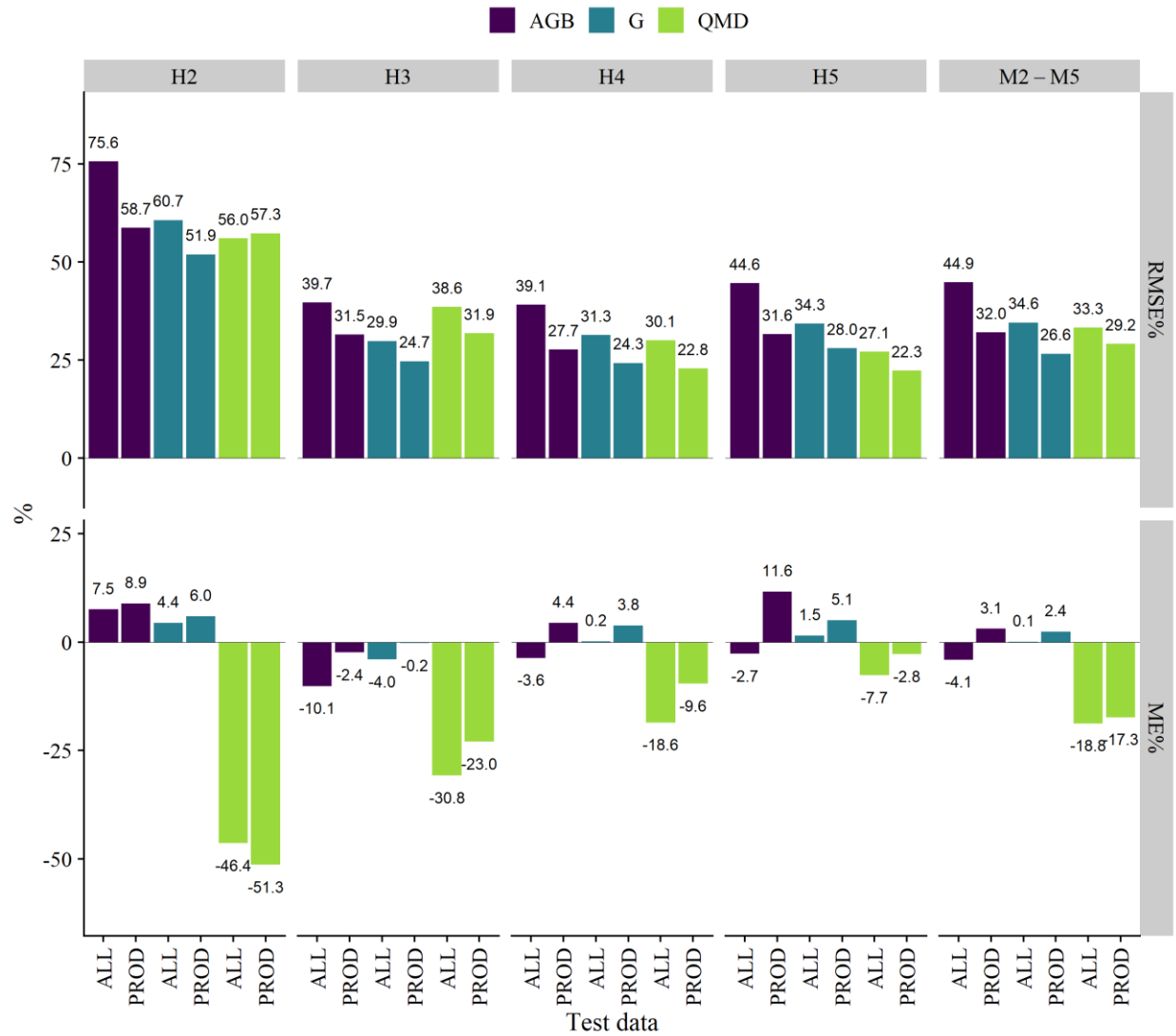
<i>Predictors</i>	AGB			G			QMD		
	<i>Estimates</i>	<i>SE</i>	<i>p</i>	<i>Estimates</i>	<i>SE</i>	<i>p</i>	<i>Estimates</i>	<i>SE</i>	<i>p</i>
(Intercept)	-45.41	5.44	<0.001	-6.22	0.97	<0.001	10.99	0.70	<0.001
hmean	15.97	0.66	<0.001	1.82	0.12	<0.001	-0.79	0.09	<0.001
d2	57.16	12.46	<0.001	23.78	2.23	<0.001	-2.60	1.05	0.013
time _{diff}	5.24	0.44	<0.001	0.66	0.08	<0.001			
h95							1.11	0.05	<0.001
RMSE%	31.17			28.89			13.99		
R^2	0.62			0.56			0.41		



16

17 **Appendix A3.** Observed versus predicted values by dominant tree species (Spruce: Norway
 18 spruce, Pine: Scots pine, Deciduous: Deciduous species) in the ALL test data.

19



20

21 **Appendix A4.** Relative root-mean-square errors (RMSE%) and mean errors (ME%) associated
 22 with the forest attribute predictions by maturity classes in the ALL and PROD test data. AGB –
 23 above-ground biomass, G – basal area, QMD – quadratic mean diameter.

24

25

26 **Appendix A5.** Characteristics associated with the estimation of forest attributes for the forest
 27 land of the study area. AGB – above-ground biomass, G – basal area, QMD – quadratic mean
 28 diameter, MA – model-assisted, SE – standard error.

Forest attribute	Direct estimate $\hat{\mu}$	2SE% $\hat{\mu}$ (%)	2SE% $\hat{\mu}_{MA}$ (%)	Systematic error of synthetic estimator $\hat{\mu}_{cor}$ (%)	Relative efficiency
AGB (t · ha ⁻¹)	80.5	1.98	1.08	-2.47	3.27
G (m ² · ha ⁻¹)	17.81	1.61	0.86	1.46	3.51
QMD (cm)	15.82	0.83	0.69	-18.77	1.45

29 **Appendix A6.** Results of MA estimators using the data and models by Hauglin et al. (2021) who
 30 used Norwegian national forest inventory and airborne laser scanning data for forest attribute
 31 mapping. Note that the study by Hauglin et al. (2021) only covered a subset of the forest land
 32 area covered by our study. However, 86 % of the plots on the forest land are the same as in our
 33 study. The same ALS data were used in both studies. The calculations given in this table are
 34 based on 6743 sample plots. For descriptions of the estimators, see Section 2.7. MA – model-
 35 assisted, SE – standard error.

Forest attribute	Direct estimate $\hat{\mu}$	2SE% $\hat{\mu}$ (%)	2SE% $\hat{\mu}_{MA}$ (%)	Systematic error of synthetic estimator $\hat{\mu}_{cor}$ (%)	Relative efficiency
HL (m)	12.72	0.89	0.32	0.31	7.85
V (m ³ · ha ⁻¹)	136.46	2.28	0.91	0.57	6.21
AGB (t · ha ⁻¹)	87.40	2.07	0.87	0.57	5.72
G (m ² · ha ⁻¹)	19.33	1.67	0.74	0.52	5.10